A Quadrupolar Superferric Magnet.

Alexandru M. Morega[1,2], *Senior Member, IEEE*, Ion Dobrin[3], Adrian Nedelcu[3], Mihaela Morega[1], *Member, IEEE*
[1] University POLITEHNICA of Bucharest, Faculty of Electrical Engineering, Bucharest, ROMANIA
[2] "Gheorghe Mihoc – Caius Iacob" Institute of Statistical Mathematics and Applied Mathematics, Romanian Academy
[3] National Institute of Electrical Engineering, ICPE-CA, Laboratory of Applied Superconductivity, Bucharest, ROMANIA
E-mail: amm@iem.pub.ro, idobrin@icpe-ca.ro, adrian.nedelcu@gmail.com, mihaela@iem.pub.ro

***Abstract*—The usage of *high temperature superconductors* (HTS) in particle accelerators of higher acceleration energy (in the TeV range) poses certain design concerns that may be conveniently addressed, in the conception phase, through mathematical modeling and numerical simulation.**

This paper presents the prototype of an YBCO superferric quadrupolar magnet for intense magnetic field of high gradient magnetic field and modeling results on the magnetic field and heat transfer. The temperature of the HTS field winding must be kept within safe limits or the HTS would exit the superconductive state. Therefore cryo-cooling provided by supercooled liquid Nitrogen is used to remove the heat influx from the ambient, which is a menace for the thermal stability of the magnet.

First, the magnetic field problem is solved for to assess the degree of uniformity of the magnetic field. Simpler, 2D models provide accurate, useful information on the magnetic field spectra. Next, the heat transfer problem, where radiation plays a major role, is solved. Two-dimensional models may not produce accurate resultsin this cases. Therefore a 3D geometry abstracted from the CAD design of the prototype was used as computational domain.

The numerical simulation results unveil the heat transfer paths within the structure that may be valuable in optimizing the design of the magnet.

Keywords: quadrupolar superferric magnet, high gradient magnetic field, thermal analysis, numerical simulation, finite element analysis.

I. INTRODUCTION

The design of particle accelerators of higher and higher acceleration energies, in the TeV range, is a major concern in high-energy physics, and any progress is related to the usage of intense magnetic fields. One of the solutions to the related technological problems might be the usage of the *high temperature superconductors* (HTS) in manufacturing the magnets for particle accelerators. In this category, the *iron core superconducting* (ICS) "superferric" magnet is used especially in applications where "wide openings"[1] for the particle flux and magnetic fields of 2 T with a high degree of uniformity ($\Delta B/B \sim 10^{-3}$) are required [1-5].

ICS magnets have higher magnetic fields and a more economic exploitation than their classical, copper coiled counterparts. Their magnetic circuits use less iron (the core has a smaller cross-section), leading to lower investment costs. Further more, the usage of HTS field windings eliminate the Joule effect and ancillary cooling system needed to exhaust the heat thus reducing the operational costs of ICS.

[1] The magnetic field zone guidance is about 150×400 mm.

Having in view that any decision on using either normal or ICS magnet boils down to cost analysis[2] and, in turn, cost analysis accounts for the lifetime of the device, the advantages of the ICS may have considerable ponder.

Depending on the magnetic field spectrum, which is required, particle accelerators utilize different types of magnets: dipole, quadrupole, sextupole, *etc*.

For wide openings and intense fields (1.7…2 T) dipolar ICS magnets with "warm" (at room temperature) iron core are best suited, as they require cooling for the superconducting coils only, thus reducing the operational cryogenic costs. The progresses registered in manufacturing cryo-coolers with two cooling stages too lead to the elimination of cryogenic agents.

This paper presents the prototype of a *quadrupole superferric magnet* (QSM) with warm iron yoke for 2 T field and 10^{-3} uniformity. The magnet is operated at 77 K, for 300 K ambient temperature. The cryo-cooling is provided by a cooling system based on Liquid Nitrogen (LN) [6]. The superconducting winding is YBCO tape stabilized with copper. The critical temperature is 92 K.

The entire experimental arrangement is contained within a stainless steel vacuumed cryostat, which provides for the thermal insulation of the superconducting coils from incoming heat flux [7]. Mathematical modeling and numerical simulation are used to analyze the magnetic field, its uniformity, and to evaluate the performance of the thermal design.

II. THE QSM PROTOTYPE

The QSM was designed to produce a high gradient magnetic field (~25 T/m) in the "hot" channel for the passage of the accelerated flow of particles. The magnetic flux density in the active part is 1.7…2 T. The prototype provides for these requirements.

A. The Prototype

Fig. 1 shows a simplified CAD projection of the QSM prototype. Several parts were removed (*e.g.*, the piping that ducts the LN, and some structural elements) for better viewing. This model is used also as computational domain in the analyses of the magnetic field and heat transfer performed by numerical simulations.

[2] A comparative analysis of the manufacturing costs was made for PANDA magnet at FAIR particle accelerator in Darmstadt [5].

Fig. 2 presents several photos that exhibit the inside part of the QSM. Fig. 2,a shows a pair of poles and, for each, one of the HTS windings coils.

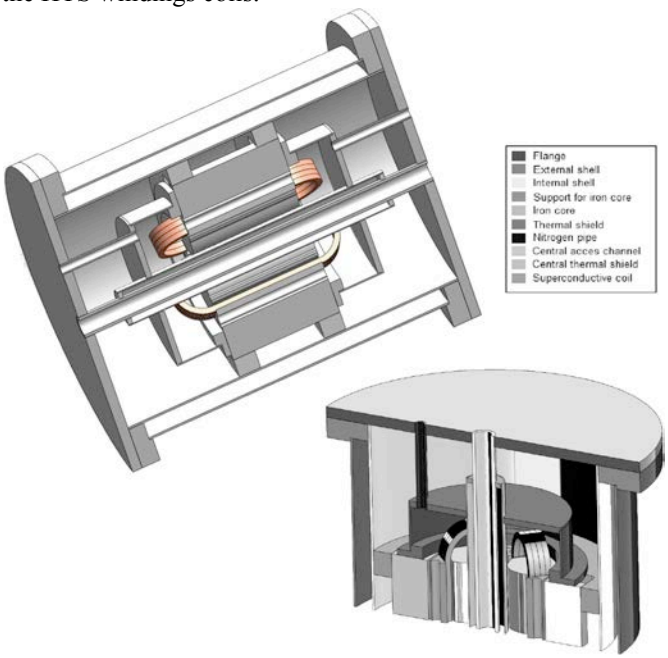

Fig. 2. CAD virtualization of the QSM used in maching the prototype and in the numerical simulations of the magnetic field and heat transfer.

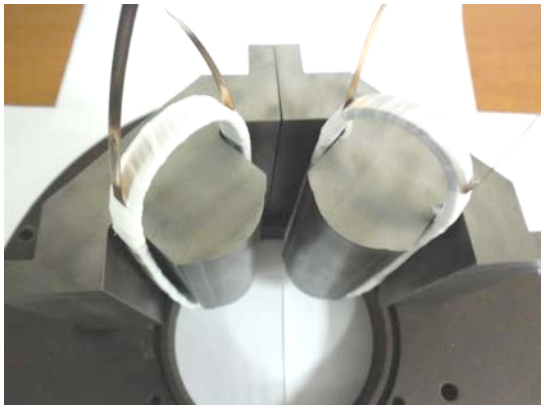

a. The iron core and coils of the YBCO HTS field windings.

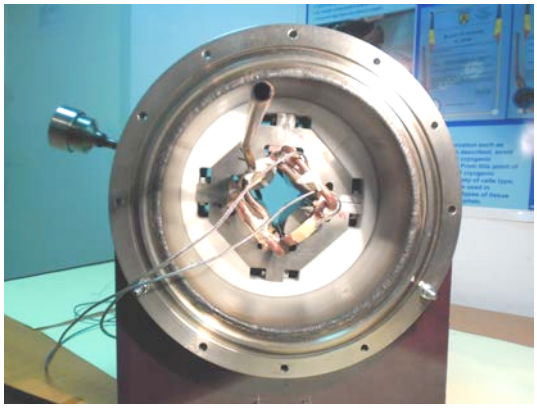

b. Front view. The enclosure is stainless steel made.

Fig. 3. The quadrupole superferric magnet prototype.

B. The Magnetic Core

The magnetic core of the QSM is made of iron without remanent magnetization. Its composition was evaluated by atomic absorption spectroscopic analysis and mass spectrometry [5]. The results evidenced that the amount of impurities does not exceed 0.92 % (99.08 % Iron) [8]. The total losses are 0.34 W/kg at 2 Hz, and 1.11 W/kg at 5 Hz. This behavior is satisfactory as that the magnet is to be operated in stationary conditions, with the slow upraise and downfall of the field current.

The magnetic pole surface has a special profile, and it is fine machined. Its design is particularly important to the linearity and uniformity of the magnetic field in the channel for the passage of accelerated particles, and its analysis makes the object of the magnetic field analysis described later.

Numerical simulations were conducted to find the core profile that provides for the desired high uniformity that the magnetic field inside the working space of the magnet has to have. CAD and finite element method (FEM) modeling were used to produce a design that was then ported for machining, and fabricated by ICPE-CA by the hot wire technology [8].

C. The QSM Cryo-Cooling System

Fig. 3 shows the quadrupole magnet and its cooling scheme that provides for suitable working conditions (77 K) for the HTS field windings.

The enclosure is a cylindrical shell fitted with two flanges made of non-magnetic stainless steel, and provided with a central passing-through duct, 20 mm in diameter, for the passage of accelerated particles, called “hot channel”. It is called “hot” because it is at ambient temperature (Fig. 1).

The enclosure is designed to provide for several important functions: it is a vacuum-proof casing of min. 10^{-5} torr, reducing the heat inflow from outside to the HTS winding; it confines and supports the iron yoke and the coils; it provides for good structural stability.

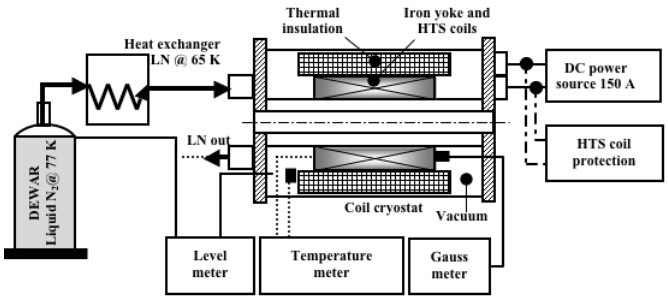

Fig. 4. The schematic of the QSM cryo-cooling system.

The iron yoke is thermally insulated from the case by supports made of Teflon. Copper thermal shields protect the coils against radiation heat transfer from the confining walls.

A problem of major concern is the thermal stability of the system because the HTS coils working temeperature must be below 90 K. The prototype uses subcooled LN to cool the superconducting winding down to 65 K. As seen in Fig. 1, LN at 77 K passes trough a heat exchanger that extracts heat

out of it, cooling it down to 65 K. LN is pumped trough a piping system for cooling the HTS coils, ant eventually exits the QSM as a single phased (liquid) fluid.

D. The HTS Field Windings

The QSM HTS field winding is made of superconducting YBCO tape. This solution provides for higher flux density magnetic field while removing the Joule losses within the field winding as the electrical resistivity of the superconductor is of the order $O(10^2)$ nΩ. This is due mainly to the normal metal-superconductor junctions. Once excited, the superconducting windings do not dissipate heat. They "trap" (prolong) the electrical current for a very long time. The critical current was measured according to the standard STAS IEC 61788-3, for the YBCO probe at 77 K (Fig. 3).

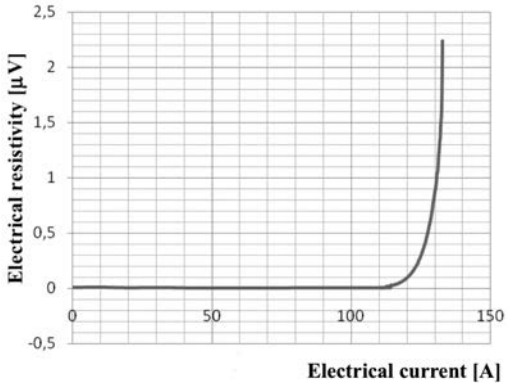

a. 5 A/min raise rate.

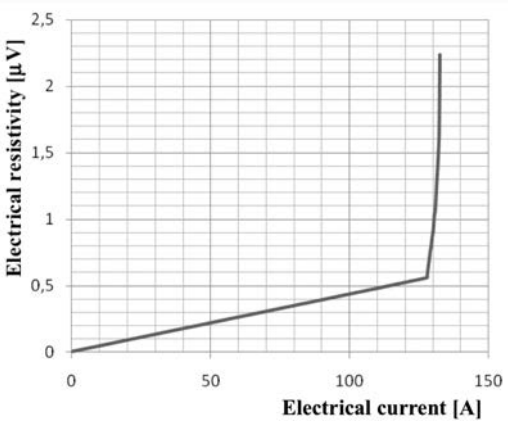

b. 1 A/min raise rate.

Fig. 5. The transition from the superconductor to the normal conductor state for different current raise rates for the YBCO tape at 77 K.

On the contrary, the losses by Joule effect dissipate a significant part (about 10 %) of the electrical power supplied to the magnet when classical, copper windings are used.

The magnetic and thermal designs of the DSM are crucial to its proper functioning, and numerical analysis proves to be a very convenient and useful tool. In what follows mathematical models and their numerical implementation are introduced. Numerical simulation results are later presented and discussed. The study is concerned with the steady state working conditions of the QSM, when all transients vanish.

III. The Mathematical Model

A. The Magnetic Field

A simpler, 2D model was used first to examine the magnetic field in a cross-sectional, vertical cut through the QSM. Next, a more complex, 3D model was built and used to investigate the magnetic field.

The magnetic field (perpendicular currents, total, gauged, magnetic vector potential) is described by the partial differential equation (PDE) [9,10]

$$\nabla \times \left(\mu_0^{-1} \mu_r^{-1} \nabla \times \mathbf{A} \right) = \mathbf{J}^e, \tag{1}$$

where $\mathbf{A}$ [T·m] is the magnetic vector potential, $\mathbf{J}^e$ [A/mm^2] is the external electrical current (in the windings), σ [S/m] is the electrical conductivity, and μ_0, $\mu_r(B)$ [H/m] are magnetic absolute and relative permeability, respectively (Fig. 5).

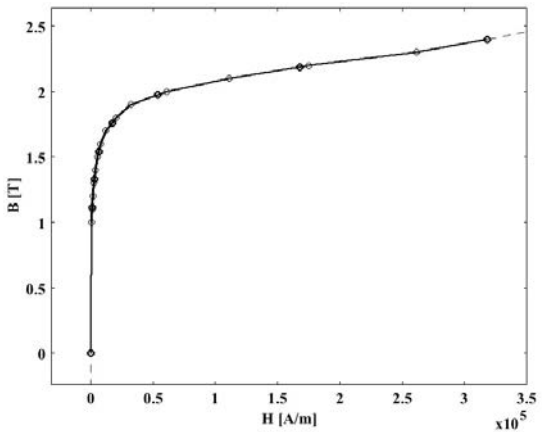

Fig. 6. The $B(H)$ curve of the QSM iron core.

Magnetic insulation ($A = 0$) boundary condition on the outer perimeter closes the model. In 2D models "infinite" elements were used to border the domain [8]. This approach leads to smaller computational domains (Fig. 3) while providing for accurate boundary conditions in open-boundary problems such the current one.

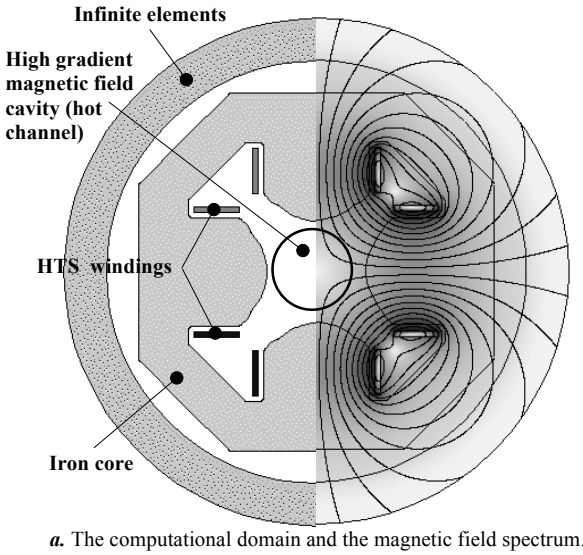

a. The computational domain and the magnetic field spectrum.

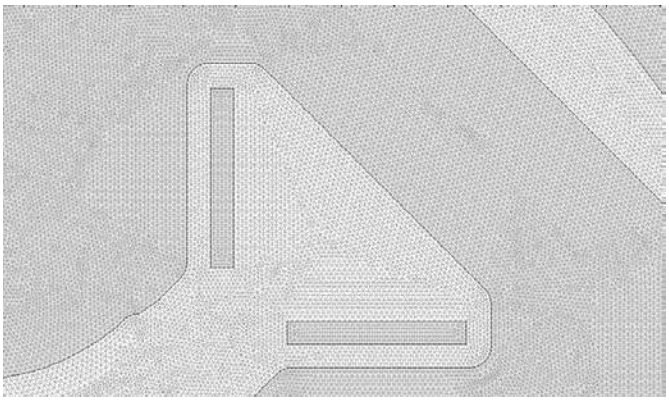

b. The 2D FEM mesh is made of *approx*. 320,000 triangular, quadratic Lagrange elements. Detail view.

Fig. 7. The 2D computational domain, magnetic flux density spectrum and FEM mesh.

The algebraic system generated by the FEM discretization of (1) was solved by using the UMFPACK solver [10]. The numerical results are shown in Fig. 7,a by magnetic flux density lines (right half) – they show the effect of using infinite elements.

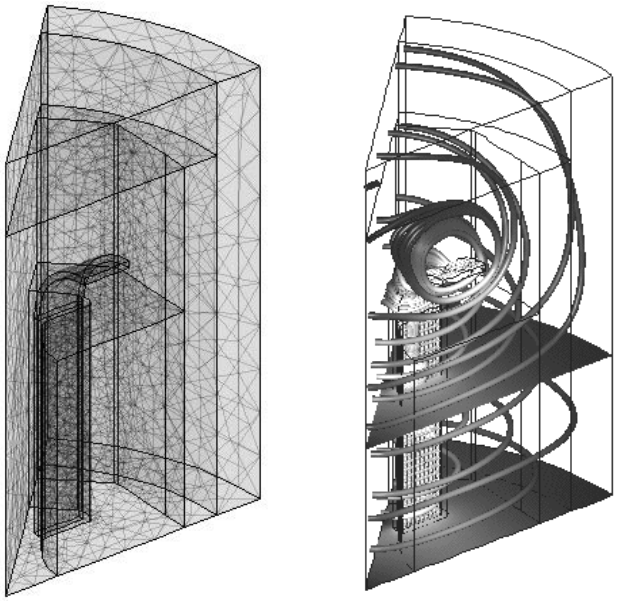

Fig. 8. The 3D model. The magnetic field is rendered through magnetic flux density stream tubes and gray map slices. The electrical current in the HTS coil is represented through arrows.

A 3D model was next considered (Fig. 7). Using the symmetry of the QSM the computational domain was greatly reduced, which resulted in higher quality (accuracy) numerical results.

The linearity of the magnetic field measures the departure of the |B| curve from linearity in radial direction. The metric is defined through

$$\varepsilon_{lin} = \left[\sum_{1}^{n} \left(B_{sim} - B_{lin} \right) \right] \Big/ n, \qquad (2)$$

where ε_{lin} is the error of linearity, B_{sim} is |B| obtained by numerical simulation, B_{lin} is the ideal curve of $|B| = f(r)$, and n is the number of points where the numerical solution was evaluated. Fig. 8 shows profiles for the magnetic pole surface.

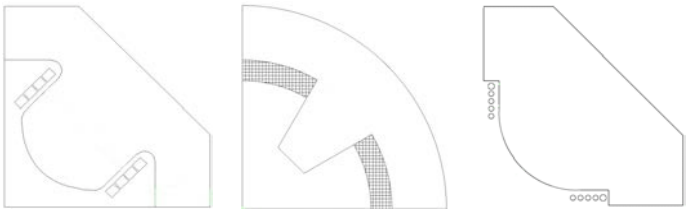

a. Current design. ***b.*** Ellipse. ***c.*** FAIR.

Fig. 9. Polar surface profiles listed in Table I.

The absolute error is defined as $\varepsilon_{abs} = \max\left(B_{sim,k} - B_{lin,k}\right)$.

The gradient of the magnetic field is given by

$$\mathrm{d}B = \left. \frac{B_k - B_{k-1}}{r_k - r_{k-1}} \right|_{k \in [2,n]}. \qquad (3)$$

The maximum value of the magnetic flux density is defined as $B_{\max} = \max\left(B_k\right)$, where $k \in [1,n]$. Table I lists several results for r = (0,15) mm, and $\theta = 45°$ (along the symmetry axes of the pole) for all cases [7].

TABLE I
NUMERICAL SIMULATION RESULTS FOR QSM. LINEARITY AND UNIFORMITY.

Index / ideal profiles	ε_{lin}	ε_{abs}[T]	dB_{med}[T]
Present QSM	0.0000721	10.4673297	0.4488104367
4 pole classical	0.002727	8.88265800	0.305477402
4 poles ellipse	0.000132	3.19974895	0.6551069541
4 poles FAIR[3]	0.000569	0.001948937	0.667088283

The linearity and the degree of uniformity of the magnetic field depend of the shape of the pole. Its profile was subject of detailed, intensive numerical analysis. The prototype provides for less than 0.3 %, the standard for QSMs [3].

B. The Heat Transfer

The QSM thermal stability is key to its successful operation. As the HTS windings operate at low temperature (below 77 K), the heat leak from the surroundings, which are at ambient temperature, has to be minimized such that the HTS temperature remains within safe operational limits.

The prototype uses a combination of forced convection heat removal methods with sub-cooled LN and radiation shielding to limit the heat influx from the ambient. A piping network channels the LN (not shown in Fig. 1, and discarded in the numerical simulations) contacts the HTS coils and bathes the presumable hot spots. LN enters at 69 K. Under QSM steady operation conditions the removed heat is less than needed for LN to reach the boiling point (90 K).

The steady state heat transfer by combined forced

[3]"Technical Report on the Design, Construction, Commissioning and Operation of the Super-FRS at the Facility for Antiproton and Ion Research ("FAIR").

convection (the HTS windings), conduction (throughout the structural parts), radiation (within the space between the case and the radiation shields), and natural convection (to the ambient) is described by the partial differential equations [11]

momentum conservation (*Navier-Stokes*) – in the cryostat

$$\rho\left[\left(\mathbf{u}\cdot\nabla\right)\mathbf{u}\right] = -\nabla p + \eta\nabla^2\mathbf{u}, \tag{4}$$

mass conservation (*incompressible flow*) – in the cryostat

$$\nabla\cdot\mathbf{u} = 0, \tag{5}$$

energy equation (*heat transfer*)

$$\rho c_p\left[\left(\mathbf{u}\cdot\nabla\right)T\right] = k\nabla^2 T, \tag{6}$$

where **u** [m/s] is the velocity (in the fluidic domain), p [N/m^2] is the pressure, T [K] is the temperature, η [N·s/m^2] is the dynamic viscosity, ρ [kg/m^3] is the mass density, k [W/(m·K)] is the thermal conductivity, and c_p [J/(kg·K)] is the specific heat[4].

There is no internal heat source because the HTS field windings operate in superconductor regime. The flow is assumed laminar, and the fluid (LN) is newtonian. In this study there is no phase change.

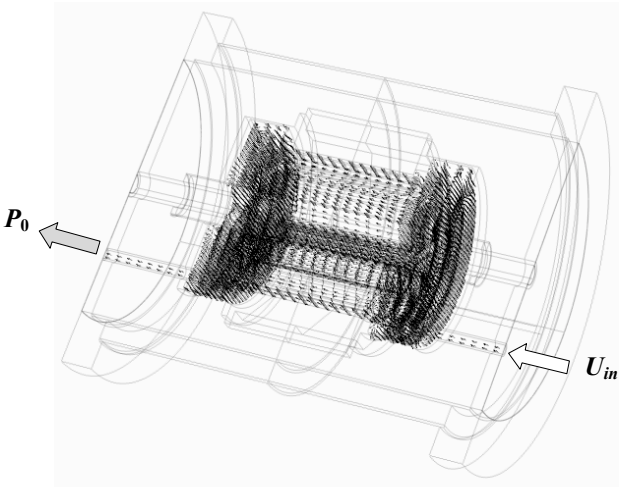

Fig. 10. The hydrodynamic problem. The flow field in the cryostat is shown through velocity vectors (arrows).

The boundary conditions for the flow are as follows: uniform velocity profile at the inlet (U_{in} = 0.01 m/s), no viscous stress at the exit, no-slip (zero) velocity at the rigid walls, and slip (zero normal velocity) at the symmetry plane.

The coupling between the flow and the heat transfer is one-way therefore the hydrodynamic problem is solved first. The mathematical model was solved by FEM technique.

The algebraic system of equations was solved with the UMFPACK solver [10]. Fig. 9 shows the velocity field through normalized arrows, for better viewing. Fig. 10 shows the flow field through streamlines. Their color is proportional to the local velocity. Using the velocity field thus found, the heat transfer problem is solved next.

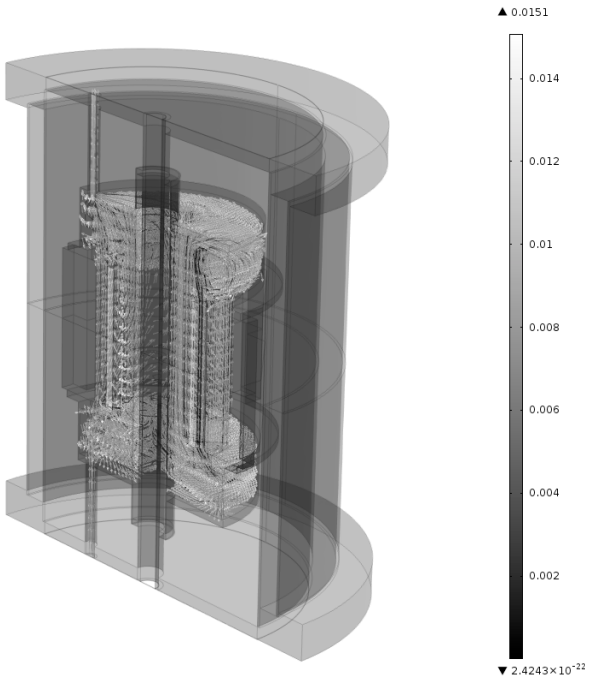

Fig. 11. LN flow in the QSM by numerical simulation. Velocity is in [m/s].

The Joule effect in the HTS field coils is negligibly small therefore the single heat source is in fact the boundary. Thermal stability has then two faces: the limitation of the heat influx from the surroundings and the evacuation of the heat that escapes inside (conduction through the structural parts, case, *etc*.). The limitation is provided by a combination of thermal shields and vacuumed layers. Thus the space between the external shell (the case) and the cryostat is vacuumed, and a radiation shield is provided within this volume (*e.g.*, Fig. 1). The heat that still escapes is collected and evacuated by the forced convection flow of LN.

As radiation heat transfer is of concern, 2D models may not produce satisfactory results. Therefore our study is based on the 3D geometry abstracted from the QSM CAD design. The steady state heat transfer by convection and, or conduction is described by (6). The BCs that close the model are as follows (Fig. 11):

The shell (*convection to the environment*)

$$-\mathbf{n}\cdot\left(-k\nabla T\right) = h\left(T_{inf} - T\right). \tag{8}$$

Symmetry plane (*adiabatic*)

$$-\mathbf{n}\cdot\left(-k\nabla T\right) = 0, \tag{9}$$

Shields surfaces

$$T = T_0, \quad (1-\varepsilon)G = J_0 - \varepsilon\sigma T^4, \tag{10}$$

where h [W/m^{2}K] is the convection heat transfer coefficient (h = 2 W/m^{2}K), ε is the surface emissivity (0.8, for all faces

[4] The physical properties for LN and the other materials are from [11].

exposed to air); T_{inf} [K] is the ambient temperature, σ is Stefan-Boltzmann constant [$5.67 \cdot 10^{-8}$ W/(m^{2}T^4)], T_0 [K] is the temperature of the mutual surface, G [W/m^2] is the incoming radiation heat flux, or irradiation, and J_0 [W/m^2] is the surface radiosity.

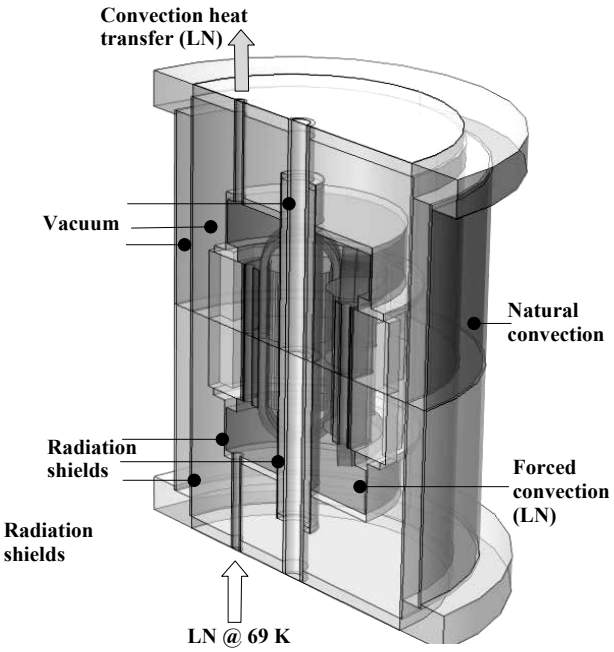

Fig. 12. The boundary conditions in the heat transfer problem.

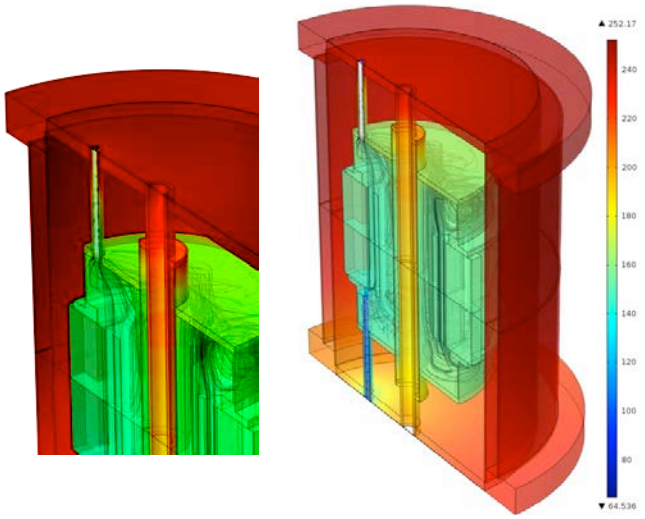

Fig. 13. The temperature field in the QSM and a zoom out – boundary color map for temperature, and streamlines (with color proportional to the local velocity) and arrows (with color proportional to the local velocity).

Fig. 12 shows the temperature of the bodies surfaces, obtained by numerical simulation. It is assumed that LN enters at 69 K and the ambient temperature is T_{inf} = 300 K. LN exits at 95 K, slightly above the boiling temperature.

The power requested by the cooler to keep the cryostat within the safe operational limits may be computed. Thus ~36 W is the heat influx through the shell (case), and ~34 W the heat carried out by LN. The HTS winding is almost isothermal, at less than 80 K. Laboratory experiments indicate 77 K.

Having in view the simplifying assumption of this 3D model, its size (*approx*. 650,000 tetrahedral Lagrange, quadratic elements), and its complexity (internal radiation heat transfer) that makes difficult extensive numerical tests, these results are within satisfactory limits of accuracy.

Interesting enough are the details provided by the numerical results about the channel. In fact, this part of the system is critical since, here, the spacing between the heat radiation screens (*i.e*., the case, the warm and cold cryostat walls) is very small, and the mutual surfaces "sees" each other at an almost 4π angle, which enhances the radiation heat transfer. Special care should be devoted in optimizing the thermal *and* magnetic design to reduce the heat leak here as much as possible.

IV. Conclusions

The paper presents the prototype of a quadrupolar superferric magnet (QSM) for particle accelerators, built with high temperature (HTS) superconductor coils. Numerical simulation results and experimental data show that the design provides a high uniformity magnetic field, in the accuracy limits generally posed to such magnets.

Mathematical modeling and FEM simulations of the magnetic field were used in the design phase of the QSM to optimize the magnetic pole profile. As result, the magnetic field magnitude, uniformity and linearity comply with the standards.

QSMs with HTS field windings require adequate cooling to ensure the thermal stability, and means and paths to diminish and convey efficiently the heat out of the system are at a prime. Although Joule effect is not of concern here, the environmental heat influx is a menace to the system stability.

The prototype is provided with internal radiation shielding, is vacuumed, and the HST winding is contained in a cryostat cooled by sub-cooled (69 K) LN forced convection. This solution provides for 77 K HTS working temperature. In steady state operation conditions LN temperature does not exceed the boiling point.

The simulations results obtained for the pumping power of the cryo-cooler are in good agreement with experimental data available.

Due attention should be given to the hot channel design. The spacing between the heat radiation screens is very small, and the mutual surfaces "see" each other under almost 4π angle.

Acknowledgment

ICPE-CA acknowledges the funding through "Core Research Program" under contract nr. 5102/2009. Numerical modeling and simulations were conducted in the Laboratory for Multiphysics Modeling at UPB.

REFERENCES

[1] G. Moritz, "Status of the development of the fair superconducting magnets", *Proceedings of EPAC 2006, Edinburgh, Scotland, 07 Accelerator Technology*, T10 Superconducting Magnets, pp. 2577-2579, 2006.

[2] F.R. Huson, J.C. Colvin, W.W. Mackay, P.M. Mcintyre, S. Pissanetzky, R.Rocha, W.M. Schmidt, G.Shotzman, J.C. Zeigler "The high field superferric magnet II", Particle Accelerators, **28**, pp. 213-218, 1990.

[3] I. Dobrin, I. Puflea, N. Stancu, S. Zamfir, "Magnet Superferic Dipolar pentru acceleratoare de particule", *Rev. EEA*, **58**, 4, pp. 39-42, 2010, ISSN 1582-5175.

[4] I. Dobrin, "Dipole Superferric Magnet", OSIM Patent request No. A/01071/2010.

[5] PANDA, http//www.gsi.de/fair/reports/btr.html/vol 3B/3.2.

[6] M. Britcliffe, T. Hanson, J. Fernandez, "A 2.5-Kelvin Gifford–McMahon/Joule–Thomson cooler for cavity maser applications", *IPN Progress Report*, Nov. 15, pp. 42-147, 2001.

[7] 5102/2009 "Core Research Programme" grant.

[8] A.M. Morega, I. Dobrin, M. Morega, "Thermal and magnetic design of a dipolar superferric magnet for high uniformity magnetic field", *Proceedings of the 7th International Symposium on Advanced Topics in Electrical Engineering*, ATEE, May 12-14, 2011, Bucharest, Romania, ISSN 2068-7966, IEEE Catalog Number CFP1114P-CDR & Porc.

[9] C.I. Mocanu, *Teoria câmpului electromagnetic*, Ed. D.P., Buc., 1980.

[10] COMSOL MultiPhysics, v. 3.5a, Comsol AB, 2010.

[11] A. Bejan, A., "*Heat transfer*," Wiley, NY, 1998.